Journal of Applied Polymer Science

Surface polarity of porous polymers at different coverages

Vladimir Yu. Gus'kov, Alina G. Ganieva, Florida Kh. Kudasheva
Bashkir State University, Ufa, Russia
Correspondence to: V. Y. Gus'kov (E-mail: guscov@mail.ru)

ABSTRACT: At different surface coverages (θs), the dispersion component (ΔF_{disp}) and specific components (induction and orientation interactions; ΔF_{io} and donor-acceptor interactions; ΔF_{da}) of the sorption free energy and the polarities were calculated for three porous polymers: the microporous styrene–divinylbenzene copolymer Dowex L-285, the microporous hypercrosslinked polystyrene MN-200, and the macroporous styrene–divinylbenzene copolymer Polysorb-1. Two methods were used to calculate ΔF_{disp}, ΔF_{io} and ΔF_{da}: the linear free energy relationship method and the Dong polarization method. For styrene–divinylbenzene sorbents, ΔF_{disp} decreased with θ, whereas ΔF_{io} and ΔF_{da} increased; this caused the polarity to rise. This phenomenon was caused by the sorbat–sorbat lateral interactions on the polymer's surface; these were stronger for polar molecules. In the case of hypercrosslinked polystyrene, ΔF_{disp} and ΔF_{io} varied equally, and the polarity was almost constant. This trend could be explained by the absorption of the molecules into the bulk of the polymer; this prevented lateral interactions. We concluded that the lateral interactions were a function of the porous polymer's surface properties. © 2016 Wiley Periodicals, Inc. J. Appl. Polym. Sci. **2016**, *133*, 44146.

KEYWORDS: adsorption; copolymers; polystyrene; porous materials; surfaces and interfaces

Received 23 February 2016; accepted 29 June 2016
DOI: 10.1002/app.44146

INTRODUCTION

The first generation of porous polymers appeared in the 1940s as gel-type copolymers of styrene with relatively small amounts of divinylbenzene (<8%). Nowadays, macroporous styrene–divinylbenzene and hypercrosslinked polystyrene polymeric sorbents are widely used (the second and third generations of porous polymers, respectively[1]. Porous polymers attract attention because of their high sorption activity and sorption capacity, their good mass transfer kinetics, the simplicity of desorption, and the ability to vary their surface chemistry and porosity.[2] The main distinction between the second and third generations of porous polymers was the improved sorption features of the latter.[3–5]

The polarity is one of the main features of any surface. In general, the term *polarity* characterizes the contribution of various intermolecular interactions to sorption energy.[6] As the impact of specific interactions increases, the surfaces become more polar. There are many ways to measure a sorbent's polarity, from the classical Rohrschneider/McReynolds method[7] to modern linear structure energy relationship (LSER) approaches.[8,9] In all methods of polarity evaluation, the experimental data are obtained at infinite dilution conditions, which correspond to the initial coverage (θ). However, there is no information about how the degree of θ influences the sorbent polarity.

Such an influence can exist because of two factors: surface heterogeneity and lateral interactions at the sorbent surface. For porous polymers, the surface heterogeneity can originate from polar sorption centers created by remnants of the polymerization initiator. In this case, as one evaluates polarity at infinite dilution conditions, the polar probes will interact with the initiator remnants, and this will lead to a higher than anticipated polarity. Polar molecules interact more strongly with each other than nonpolar molecules, and this will lead to more intense lateral interactions.

One of the most informative methods for determining the polarity of porous polymers is inverse gas chromatography. With this valuable tool, major surface characteristics, such as the surface energy and polarity,[10,11] and Flory–Huggins interaction parameters,[12] can be measured. In this article, we present a comprehensive study of the polarity of three porous polymers and different intermolecular interactions between the probe and each polymer's surface by inverse gas chromatography.

EXPERIMENTAL

Porous Polymers

The porous polymers Dowex L-285 (Dow Chemicals), Polysorb-1 (Russia), and MN-200 (Purolite, United Kingdom) were used in this study. Their specific surface areas were 800, 250, and

Additional Supporting Information may be found in the online version of this article.

900 m^2/g, respectively. The average pore sizes were 25 and 130 Å for Dowex L-285 and Polysorb-1, respectively. MN-200 is a biporous sorbent with an average micropore size of about 15 Å and an average macropore size of about 800 Å.

Gas Chromatography

The sorbents studied were packed in stainless steel columns measuring 500 × 3 mm. A Chrom 5 gas chromatograph (Laboratorni Pristroje, Czech Republic) equipped with a thermal conductivity detector was used. The column temperature was maintained at 200 °C. Experiments were conducted at this high temperature because of the strong sorbate retention for the sorbents studied. The nitrogen carrier gas flow rate was 30 mL/min. Probes were injected as liquid samples with volumes from 0.02 to 70 µL. All samples were conditioned overnight at 200 °C.

Hexane, heptane, octane, benzene, toluene, ethanol, *n*-propanol, *n*-butanol, *i*-propanol, *i*-butanol, and ethyl acetate were used as sorbates capable of different intermolecular interactions.

Calculations

From the experimental data, the values of the specific retention volume [$V^0_{g(T)}$; mL/g] were obtained. The peak desorption branches obtained at the same flow rate were superimposed; this allowed us to consider sorption processes in the column that were close to ideal chromatography and to equate $V^0_{g(T)}$ with the sorption–desorption equilibrium constant. In the case of infinite dilution conditions, the interactions between probe molecules were absent, and the sorption–desorption equilibrium constant was equal to Henry's constant.[13]

Differential isoteric free energies ($-\Delta F$s, kJ/mol) of sorption were calculated as follows:

$$\Delta F = -RT \ln V^0_{g(T)} \quad (1)$$

where R universal gas constant, T temperature.

The sorption isotherms for each probe injection volume were calculated according to the classical Gluckauf approach.[14] These isotherms correspond well with those generated by the Langmuir equation (see Supporting Information). The Langmuir equation was used to calculate θ values from the isotherms.

To obtain ΔF for identical θ values, we plotted $V^0_{g(T)}$ versus θ. These plots were fitted by polynomial regression analysis. The calculated fits described the experimental data with correlation coefficient r greater than 0.99, and the curves exhibited no deviation from the data points [an example of the curves generated by these fits is shown in Figure 1. All data for $V^0_{g(T)}$ versus θ are provided in the Supporting Information].

From the previous equations, ΔF was calculated from zero to maximal θ in increments of 0.02 where data was available. For Dowex L-285, MN-200, and Polysorb-1, the maximal θs were 0.4, 0.3 and 0.28, respectively. Subsequently, the ΔF_{disp} and ΔF_{io} measurement were determined at each θ.

Because any approach for calculating the polarity is based on a model with some assumptions, we used two independent methods to measure the intermolecular interactions energies and surface polarity.

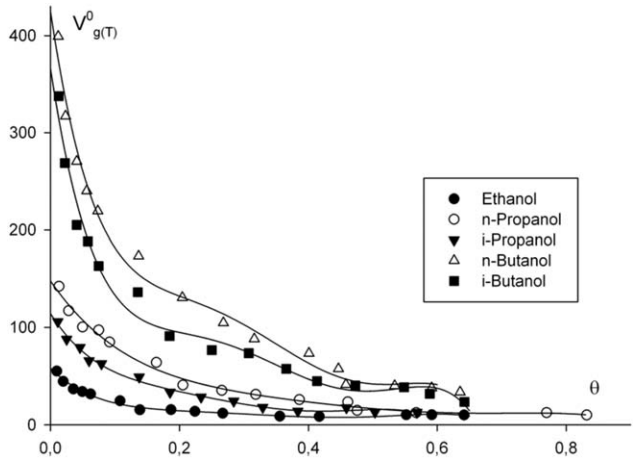

Figure 1. $V^0_{g(T)}$ versus the surface θ for alcohols on the porous polymer MN-200.

The first method was based on the broadly used linear free energy relationship (LFER) approach.[6,8,9,15–17] In this method, the free sorption energy was divided into a few components, each of which characterized the free energy of one of the intermolecular interactions and could be referred to as the product of the surface properties coefficient and the characterized probe properties descriptor. The latter descriptors were tabulated. Then, the surface coefficients were calculated for a set of probes by multiple-regression analysis. From the data obtained, the free energy from different types of intermolecular interactions of the sorption were calculated, and a comparison of the surface polarities were made.

In this study, the Larionov LFER equation[16] was used, according to Ref. 18. The sorption free energy could be divided into dispersion (ΔF_{disp}), specific (ΔF_{io}), and donor–acceptor components (ΔF_{da}):

$$\Delta F = \Delta F_{disp} + \Delta F_{io} + \Delta F_{da} \quad (2)$$

Each of these was expressed as the product of a surface coefficient with an unknown value and a probe descriptor with a known value:

$$-\Delta F_{disp} = K_1 \alpha_B + K_5 \quad (3)$$

$$-\Delta F_{io} = K_2 \left(\frac{2\mu_B^2}{3kT} + \alpha_B \right) \quad (4)$$

$$-\Delta F_{da} = K_3 W_B^{\alpha} + K_4 W_B^{d} \quad (5)$$

where K_1, K_2, K_3, and K_4 are the coefficients characterized by the sorbent surface properties dispersion, induction and orientation, electron donor, and electron acceptor, respectively. The coefficient K_5 also characterizes the dispersion interactions.[6,8] The molecular descriptors used were the polarizability, dipole moment, electron-acceptor, and electron-donor constants of the sorbate (α_B, μ_B, W_B^{α}, and W_B^{d}, respectively); k is the Boltzmann constant; and T is the temperature (K). The values of α_B, μ_B, W_B^{α}, and W_B^{d} have been tabulated and reported in the literature. From eqs. (2–5), the general LFER equation could be expressed as follows:

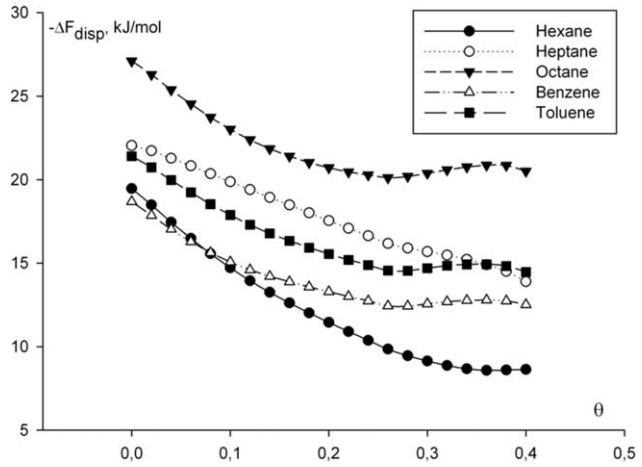

Figure 2. $-\Delta F_{disp}$ versus θ for hexane, heptane, octane, benzene, and toluene on Dowex L-285 (LFER method).

$$-\Delta F = K_1\alpha_B + K_2\left(\frac{2\mu_B^2}{3kT} + \alpha_B\right) + K_3 W_B^{\alpha} + K_4 W_B^{d} + K_5 \quad (6)$$

ΔF as a function of θ was obtained from the experimental data, and calculations were performed as described previously. This allowed us to write an eq. (6) for each probe used (where the coefficients K_1–K_5 were unknown values) and to solve this set of equations by multiple-regression analysis.

The second method was based on the division of the sorption free energy upon dispersion $\Delta F'_{disp}$ into specific ($\Delta F'_{spec}$) components according to the following equation:

$$\Delta F = \Delta F'_{disp} + \Delta F'_{spec} \quad (7)$$

In this method, $\Delta F'_{spec}$ includes the induction, orientation, and donor–acceptor interactions. We assumed that the alkanes were only capable of dispersion interactions. Therefore

$$\Delta F_{alkanes} = \Delta F'_{disp,alkanes} \quad (8)$$

where $\Delta F_{alkanes}$ is the total alkanes adsorption energy and $\Delta F'_{disp,alkanes}$ is the dispersion component of alkanes adsorption energy. For polar molecules, ΔF_{disp} could be easily calculated from the reference line of $\Delta F_{alkanes}$ versus any appropriate physicochemical property dependence.[19,20] In this study, we used the polarizability method proposed by Dong *et al.*,[21] whereby ΔF_{disp} is taken to be the sorption free energy of a hypothetical alkane with the same polarizability. ΔF_{io} can be calculated as the difference between the total sorption free energy and ΔF_{disp}.

The average impact of ΔF_{spec} and ΔF_{da} on ΔF is used as a surface polarity parameter (P) to compare polarities at different θs:

$$P = \frac{\sum\left(\frac{\Delta F^n_{spec} + \Delta F^n_{da}}{\Delta F_n}\right)}{n_{probes}} \times 100\% - P_{GCB} \quad (9)$$

where n_{probes} is the number of sorbates, ΔF_n, ΔF^n_{spec} and $\Delta F^n{}_{da}$ are the total, specific and donor-acceptor components of sorption energy for one of n sorbates. P for graphitized carbon black P_{GCB} was used as a reference.

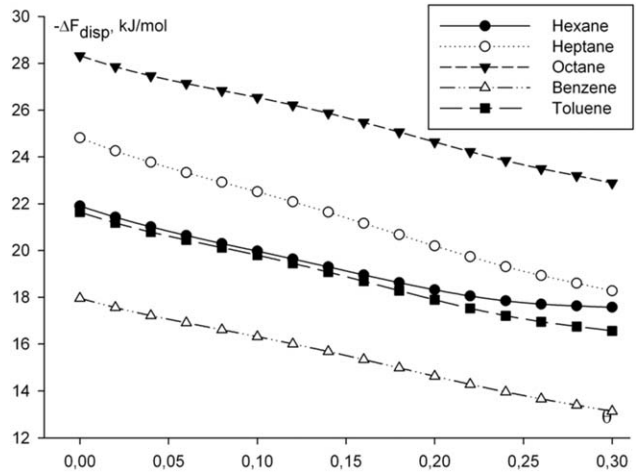

Figure 3. $-\Delta F_{disp}$ versus θ for hexane, heptane, octane, benzene, and toluene on MN-200 (LFER method).

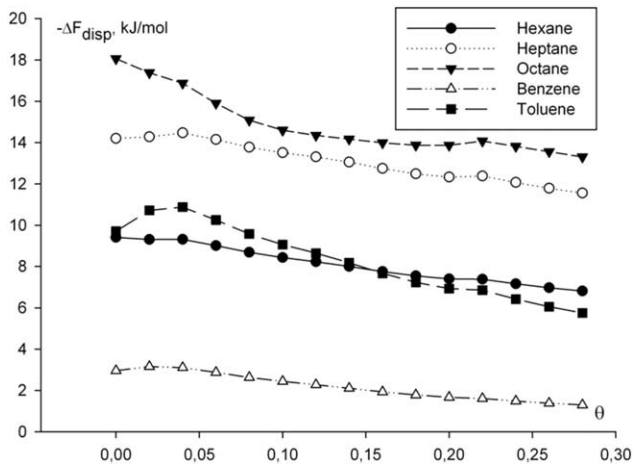

Figure 4. $-\Delta F_{disp}$ versus θ for hexane, heptane, octane, benzene, and toluene on Polysorb-1 (LFER method).

RESULTS AND DISCUSSION

Intermolecular Interaction Energies Determined with the LFER Method

In Figures 2–7, the dependence of ΔF_{disp} on θ is shown. For all sorbents, ΔF_{disp} generally decreased as θ increased. This trend

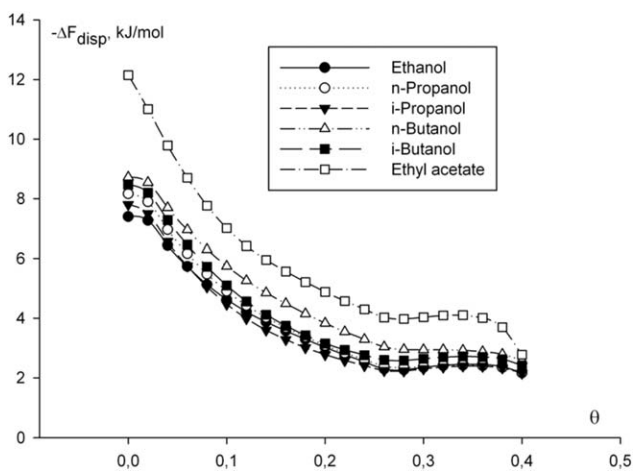

Figure 5. $-\Delta F_{disp}$ versus θ for ethanol, *n*-propanol, *i*-propanol, *n*-butanol, *i*-butanol, and ethyl acetate on Dowex L-285 (LFER method).

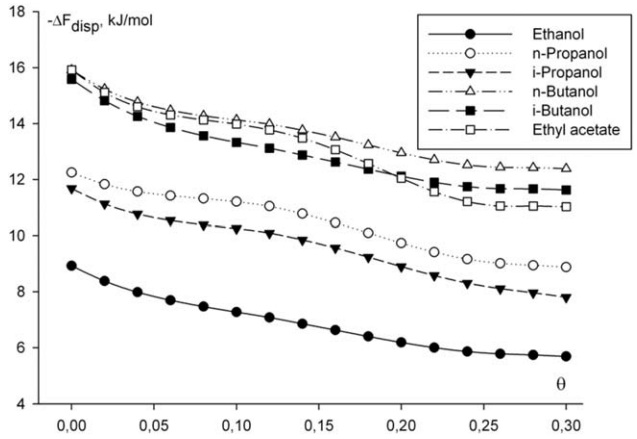

Figure 6. $-\Delta F_{disp}$ versus θ for ethanol, *n*-propanol, *i*-propanol, *n*-butanol, *i*-butanol, and ethyl acetate on MN-200 (LFER method).

could be explained by the condensation approximation approach, which states that molecules will be adsorbed on the sorption centers of maximal energy;[11] in the case of dispersion interactions, these were the pores with the smallest dimension. As θ increased, the pore size in which the sorption of organic molecules occurred increased; this led to the decay of dispersion interactions.

For Dowex L-285, at θ values greater than 0.26–0.28, the ΔF_{disp} values were constant. This phenomenon could be explained by probe sorption into the macropores. For other sorbents, this phenomena was not observed; this was likely due to the micropore–mesopore–macropore ratio because sorption in macropores only occurred at θ values higher than those available in our experiment.

It is noteworthy that for some probes, the curves of $-\Delta F_{disp}$ versus θ were different for each sorbent. In the case of Dowex L-285 (microporous styrene–divinylbenzene), the curves for benzene and hexane were superimposed at low θ, whereas at high θ, the benzene curve was above the hexane curve. At the same time, most of the toluene curve was below that of the heptane curve. However, for MN-200 (microporous hypercrosslinked polystyrene) and Polysorb-1 (macroporous styrene–divinylbenzene), the inverse relationship was observed: the hexane and heptane curves were above the benzene and toluene curves, respectively. This trend was typical, given that the polarizabilities of hexane and heptane were higher than those of benzene and toluene, respectively.

In the case of Dowex L-285, the observed phenomena were caused by high benzene and toluene absorption in the bulk. This additional parameter was not accounted for in the LFER method. For Polysorb-1, this phenomenon was not specific, whereas for MN-200, the absorption of all molecules in the bulk was observed.

For alcohols on Dowex L-285, the curves of $-\Delta F_{disp}$ versus θ were superimposed, whereas for MN-200 and Polysorb-1, $-\Delta F_{disp}$ increased with the number of carbon atoms in the homologous series. This increase was notably higher for MN-200 than for Polysorb-1; this could have been caused by different sorption mechanisms on the polymer surfaces.

Dowex L-285 is a microporous sorbent for which sorption occurs according to the theory of micropore filling. In the case of alcohols, it is likely that robust associations with the surface are formed. Macroporous sorption is typical for Polysorb-1, so the sorption mechanism is different. In the case of MN-200, molecules can absorb in the polymer bulk.

Figures 8–13 and 14–16 show $-\Delta F_{io}$ and $-\Delta F_{da}$ versus θ, respectively. For Dowex L-285, $-\Delta F_{io}$ increased noticeably up to a θ of 0.26 for alkanes and arenes and then varied slightly when θ was greater than 0.26. Alcohols exhibited a modest increase up to a θ of 0.26 followed by a decrease at high values of θ.

There was a noticeable increase in $-\Delta F_{da}$ up to a θ of 0.26 for arenes and alcohols. At θs greater than 0.26, the energy of donor–acceptor interactions was almost constant.

Polysorb-1 exhibited a general increase in $-\Delta F_{da}$ and $-\Delta F_{io}$ as θ increased, but at extremely low θs ($0 < \theta < 0.06$), $-\Delta F_{io}$ and $-\Delta F_{da}$ decreased, the latter at about 3 kJ/mol (almost to zero).

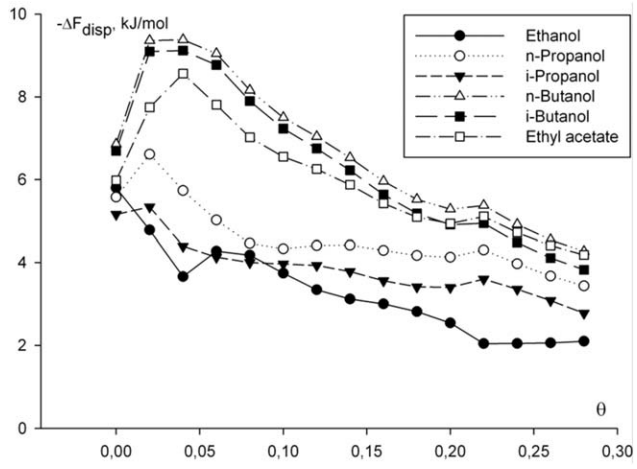

Figure 7. $-\Delta F_{disp}$ versus θ for ethanol, *n*-propanol, *i*-propanol, *n*-butanol, *i*-butanol, and ethyl acetate on Polysorb-1 (LFER method).

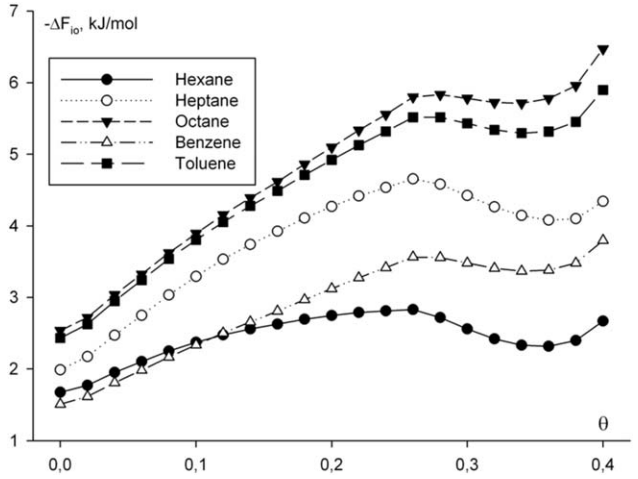

Figure 8. $-\Delta F_{io}$ versus θ for hexane, heptane, octane, benzene, and toluene on Dowex L-285 (LFER method).

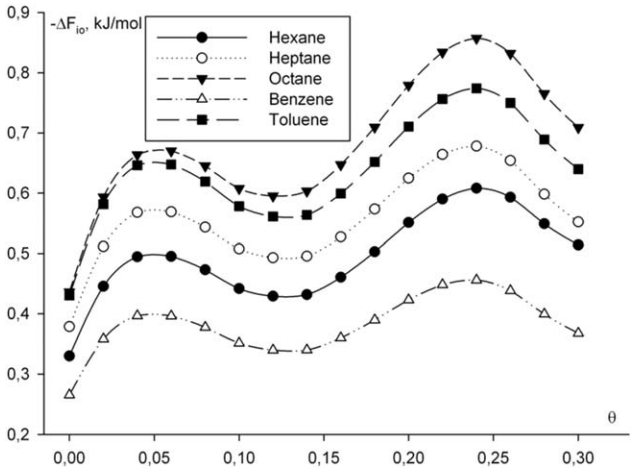

Figure 9. $-\Delta F_{io}$ versus θ for hexane, heptane, octane, benzene, and toluene on MN-200 (LFER method).

Most likely, this phenomenon was caused by the presence of polar sorption centers from remaining polymerization initiators.

All of the discussed phenomena had an effect on the sorbent polarity (see Figure 17). For Dowex L-285, the polarity linearly increased up to a θ of 0.26 and then plateaued. The main impact of alcohols on the polarity increase occurred via donor–acceptor interactions; for arenes, the impact of $-\Delta F_{da}$ and $-\Delta F_{io}$ was approximately equal (the $-\Delta F_{da}$ value for arenes also characterized the π–π interactions with the polymer benzene rings).

For Polysorb-1, polarity decreased with θ when θ was less than 0.06 but exhibited a linear increase when θ was 0.06 or greater. It was interesting to note that the degree to which the polarity increased was almost equal for Dowex L-285 and Polysorb-1: the *P* versus θ slope was 116 for Dowex L-285 and 125 for Polysorb-1 with correlation coefficient (*r*) values of 0.979 and 0.985, respectively.

We concluded that the polarity increase for Dowex L-285 and Polysorb-1 was due to lateral interactions because they became

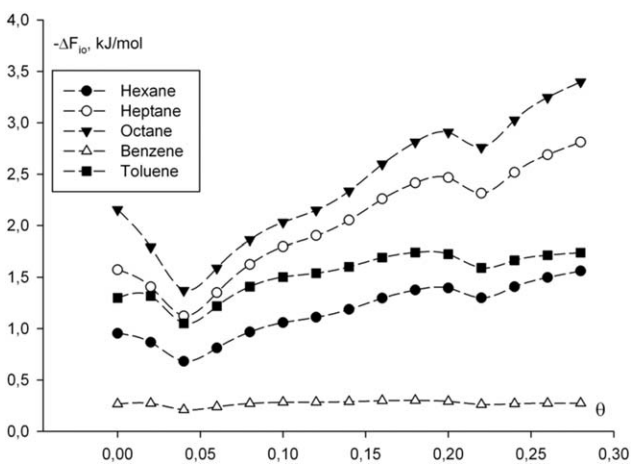

Figure 10. $-\Delta F_{io}$ versus θ for hexane, heptane, octane, benzene, and toluene on Polysorb-1 (LFER method).

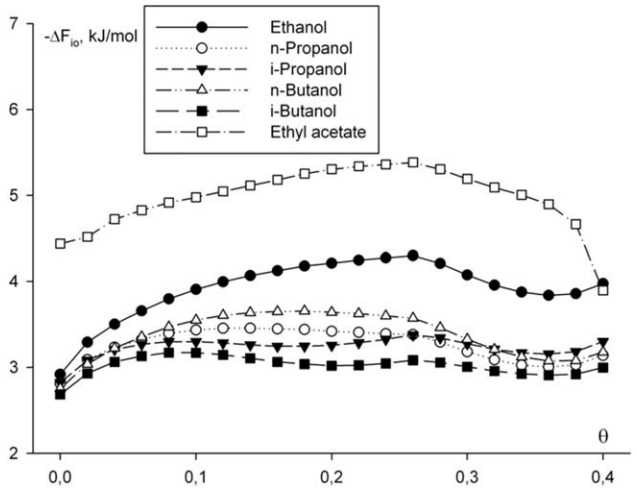

Figure 11. $-\Delta F_{io}$ versus θ for ethanol, *n*-propanol, *i*-propanol, *n*-butanol, *i*-butanol, and ethyl acetate on Dowex L-285 (LFER method).

stronger as θ increased. For alcohols, such interactions were significantly stronger than for alkanes. Lateral interactions were the cause of higher retention volumes for the alcohols with respect to the alkanes; this led to an increase in the polarity. In the *P* versus θ plot (Figure 17), the curve for Polysorb-1 was below that for Dowex L-285.

It was linked to the Polysorb-1 porosity: a higher average pore size decreased the probability for lateral interactions. In the micropores of Dowex L-285, the space between molecules was significantly smaller than the macropores of Polysorb-1; this led to strong lateral interactions, even at low θ.

It was notable that for Dowex L-285, at low θ, the benzene curve was superimposed on the hexane curve, whereas at high θ, the benzene curve was above it (Figure 8). By contrast, for Polysorb-1, the benzene curve was noticeably below hexane curve (Figure 10). Similar dependencies were observed for toluene and heptane. Together, these data demonstrated the stronger π–π interactions of arenes with the Dowex L-285 surface, which were supplemented by π–π lateral interactions at high θ.

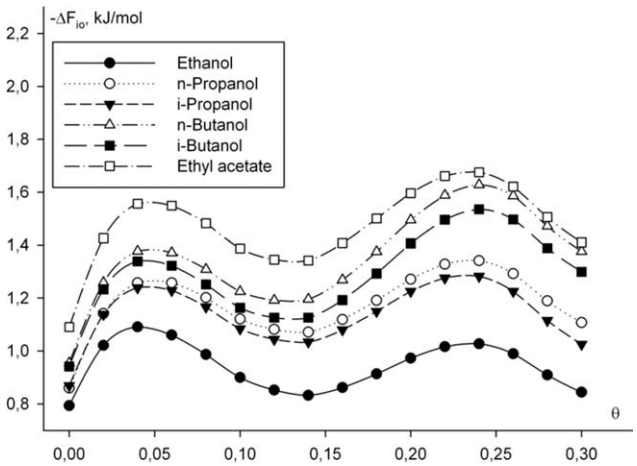

Figure 12. $-\Delta F_{io}$ versus θ for ethanol, *n*-propanol, *i*-propanol, *n*-butanol, *i*-butanol, and ethyl acetate on MN-200 (LFER method).

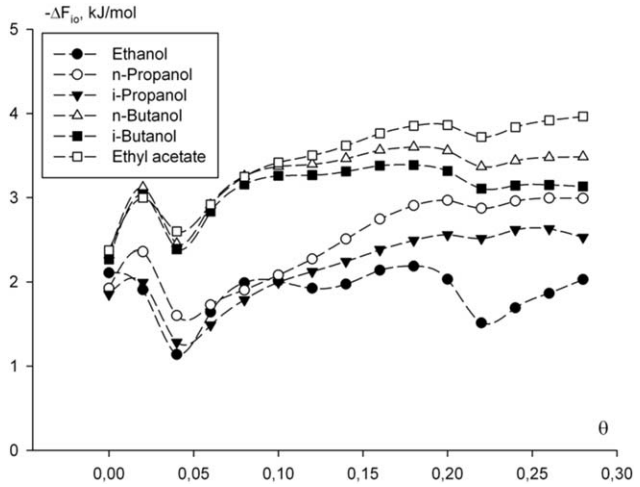

Figure 13. $-\Delta F_{spec}$ versus θ for ethanol, *n*-propanol, *i*-propanol, *n*-butanol, *i*-butanol, and ethyl acetate on Polysorb-1 (LFER method).

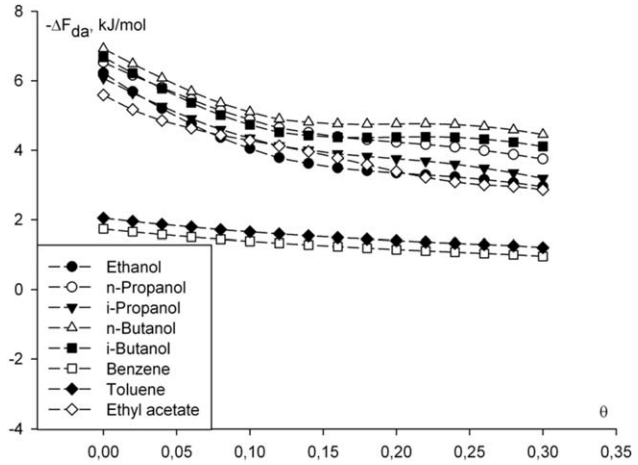

Figure 15. $-\Delta F_{da}$ versus θ for ethanol, *n*-propanol, *i*-propanol, *n*-butanol, *i*-butanol, and ethyl acetate on MN-200 (LFER method).

For the microporous hypercrosslinked polystyrene MN-200, the $-\Delta F_{io}$ values for alkanes and arenes were less than 1 kJ/mol and almost constant. The $-\Delta F_{io}$ for alcohols was also virtually constant.

It was noteworthy that for benzene and toluene, the $-\Delta F_{da}$ values were constant, whereas for alcohols and ethyl acetate, they decreased about 2 kJ/mol. This dependence led to constant values for the MN-200 polarity (Figure 17) and could be explained by primary absorption in the polymer bulk. The term *surface* was not correct for this sorbent. The sorbate molecules were absorbed separately from one another in the 3D polymeric network; this disabled lateral interactions. As the result, if at infinite dilution conditions Dowex L-285 and MN-200 had the same polarity, at θ values greater than 0.04, the latter behaved as if it were less polar.

Intermolecular Interaction Energies Determined with the Dong Method

The analysis of our data via the Dong method[21] exhibited results similar to those of analysis by the LFER method (see the Supporting Information). For Dowex L-285, ΔF_{disp} decreased with θ, and ΔF_{io} increased in a manner similar to that observed with the previous method. For Polysorb-1, ΔF_{disp} increased for some sorbates up to a θ of 0.1 and decreases when θ was greater than 0.1 for all probes. At the same time, the variation in ΔF_{io} was insignificant. For MN-200, both ΔF_{disp} and ΔF_{io} decreased; this led to an invariable polarity. Thus, the conclusions obtained from the analysis via the Dong method confirmed the conclusions from the analysis via the LFER method (see the Intermolecular Interaction Energies Determined with the LFER Method section).

CONCLUSIONS

We determined that for porous polymers ΔF_{disp}, ΔF_{io}, and the polarity were functions of θ. In the case of styrene–divinylbenzene porous polymers (second generation), ΔF_{disp} decreased and ΔF_{io} increased with θ; this led to an enhancement in the surface polarity. In the case of Polysorb-1, when θ was less than 0.06, the polarity decreased notably with θ because of the polar sorption centers were generated by remnants of the

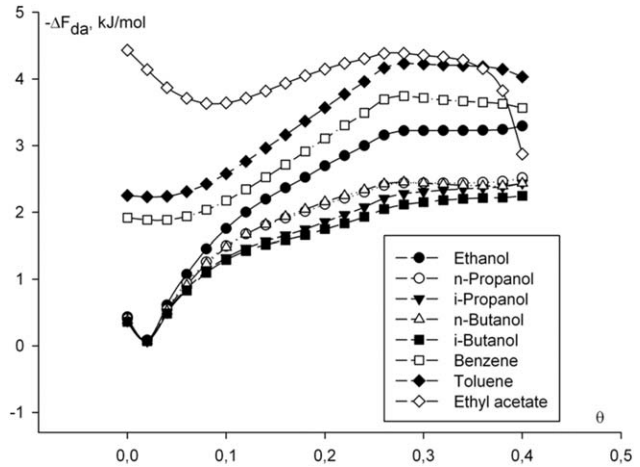

Figure 14. $-\Delta F_{da}$ versus θ for ethanol, *n*-propanol, *i*-propanol, *n*-butanol, *i*-butanol, and ethyl acetate on Dowex L-285 (LFER method).

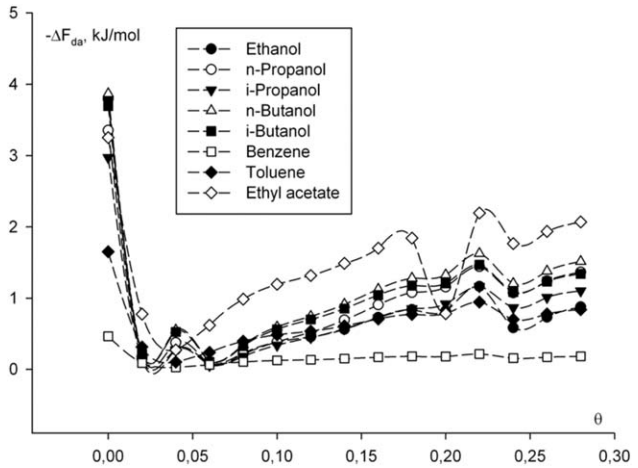

Figure 16. $-\Delta F_{da}$ versus θ for ethanol, *n*-propanol, *i*-propanol, *n*-butanol, *i*-butanol, and ethyl acetate on Polysorb-1 (LFER method).

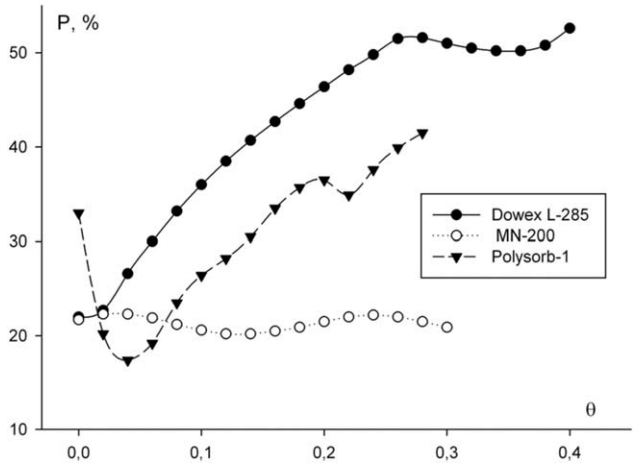

Figure 17. *P* versus θ.

polymerization initiator. The polarity for the hypercrosslinked polystyrene (third generation) was almost constant at all values of θ studied.

The observed phenomena could be explained by the presence of sorbat–sorbat lateral interactions with the surface of the porous polymers. As θ increased, so did the possibility for lateral interactions. The energy of these interactions was much stronger for polar molecules than for nonpolar molecules; this resulted in an increased retention of polar compounds with respect to nonpolar compounds on the surface of the styrene–divinylbenzene porous polymers. For sorbents with a lower average pore size, the potential for lateral interactions was higher. The Dowex L-285 polarity increased with respect to Polysorb-1 when θ was greater than 0.02. In the case of the porous polymer MN-200, however, the absorption to the polymer bulk prevented any lateral interactions.

Thus, ΔF_{disp}, ΔF_{io}, and the polymer's polarity varied as functions of θ. Importantly, this dependence was distinct for different porous polymers. The real final polarity was a property of the layer of molecules adsorbed onto the polymer surface. However, the last one was a function of the sorbent surface, so the matrix and porosity of the polymers could alter the behavior of the sorbate with the polymer surface. The approach outlined in this article could be helpful if one wishes to optimize their choice of porous polymers for use in purification processes, solid-phase extraction, preparative chromatography, catalysis, and other applications that use porous polymers under conditions where θ does not tend toward zero.

ACKNOWLEDGMENTS

This work was partially supported by the Basic Research Task of the Ministry of Education and Science of the Russian Federation (project 2522). The authors are grateful to V. A. Davankov for providing the MN-200 samples.

REFERENCES

1. Davankov, V.; Tsyurupa, M.; Ilyin, M.; Pavlova, L. J. *Chromatogr. A* **2002**, *965*, 65.
2. Maciejewska, M.; Szajnecki, Ł.; Gawdzik, B. *J. Appl. Polym. Sci.* **2012**, *125*, 300.
3. Tsyurupa, M. P.; Maslova, L. A.; Andreeva, A. I.; Mrachkovskaya, T. A.; Davankov, V. A. *React. Polym.* **1995**, *25*, 69.
4. Zhai, Z. C.; Chen, J. L.; Fei, Z. H.; Wang, H. L.; Li, A. M.; Zhang, Q. X. *React. Funct. Polym.* **2003**, *57*, 93.
5. Long, C.; Yu, W.; Li, A. *Chem. Eng. J.* **2013**, *221*, 105.
6. Gus'kov, V. Y.; Kudasheva, F. K.; Mozgovoi, O. S. *Prot. Met. Phys. Chem. Surf.* **2013**, *49*, 639.
7. McReynolds, W. O. Gas Chromatographic Retention Data; Preston Technical Abstracts: Evanston, IL, **1966**.
8. Vitha, M.; Carr, P. W. *J. Chromatogr. A* **2006**, *1126*, 143.
9. Laffort, P. *J. Chromatogr. A* **2011**, *1218*, 4025.
10. Ho, R.; Sun, Y.; Chen, B. *J. Appl. Polym. Sci.* **2015**, *132*, DOI: 10.1002/app.41679.
11. Mills, R. H.; Tze, W. T. Y.; Gardner, D. J.; Van Heiningen, A. *J. Appl. Polym. Sci.* **2008**, *109*, 3519.
12. Huang, J.-C. *J. Appl. Polym. Sci.* **2013**, *127*, 5000.
13. Grajek, H. *J. Chromatogr. A* **2003**, *986*, 89.
14. Gluckauf, E. *Nature* **1945**, *156*, 748.
15. Park, J. H.; Lee, Y. K.; Donnet, J. *B. Chromatographia* **1992**, *33*, 154.
16. Larionov, O. G.; Petrenko, V. V.; Platonova, N. P. *J. Chromatogr. A* **1991**, *537*, 295.
17. Huang, J.-C. *J. Appl. Polym. Sci.* **2012**, *124*, 1295.
18. Gus'kov, V. Y.; Gainullina, Y. Y.; Ivanov, S. P.; Kudasheva, F. K. *J. Chromatogr. A* **2014**, *1356*, 230.
19. Kondor, A.; Quellet, C.; Dallos, A. *Surf. Interface Anal.* **2015**, *47*, 1040.
20. Praveen Kumar, B.; Ramanaiah, S.; Madhusudana, T.; Reddy, K. S. *Surf. Interface Anal.* **2016**, *48*, 4.
21. Dong, S.; Brendle, M.; Donnet, J. *B. Chromatographia* **1989**, *28*, 469.